Analytica Chimica Acta, 227 (1989) 37–48
Elsevier Science Publishers B.V., Amsterdam — Printed in The Netherlands

PRE-CHEMILUMINESCENT BIEXPONENTIAL DEGRADATION OF BIS(2,4-DINITROPHENYL) OXALATE IN HYDROGEN PEROXIDE–ACETONITRILE

R.N. JENNINGS* and ANTHONY C. CAPOMACCHIA

Department of Pharmaceutics, College of Pharmacy, University of Georgia, Athens, GA 30602 (U.S A.)

(Received 2nd August 1989)

SUMMARY

The pre-chemiluminescent hydrogen peroxide–bis(2,4-dinitrophenyl) oxalate reaction has been studied in order to understand better its role in peroxyoxalate chemiluminescence. The reaction is shown to be first order in each reactant. An unusual biexponential degradation of the oxalate occurs which suggests that it exists in solution as two conformations that react with hydrogen peroxide at different rates. Inclusion of the fluorophor 9,10-diphenylanthracene does not affect the reaction rate.

Chemiluminescence (CL) from the reaction of aryl oxalate esters such as bis(2,4-dinitrophenyl) oxalate (DNPO), hydrogen peroxide and a fluorophore (F) has been postulated to occur by means of the following general reaction scheme [1,2]:

$$\text{oxalate ester} + \text{HOOH} \longrightarrow \text{reactive intermediate (RI)} + \text{products} \quad (1)$$

$$\text{RI} + \text{F} \longrightarrow \text{RI–F or } \text{RI}^{-\cdot}\text{F}^{+\cdot} \quad (2)$$

$$\text{RI–F or } \text{RI}^{-\cdot}\text{F}^{+\cdot} \longrightarrow {}^1\text{F} + \text{products} \quad (3)$$

$${}^1\text{F} \longrightarrow h\nu\ (\text{CL}) + \text{F} \quad (4)$$

The scheme was developed from experimental measurements of CL intensity, quantum efficiency, reaction rates and rate constants, under a variety of experimental conditions [1–8]. The importance of the relative stoichiometry between oxalate ester and HOOH has also been investigated [1,9,10]. Other than the latter there are no published studies on the pre-CL dark reaction between oxalate ester and HOOH (Eqn. 1 in the above scheme), despite recent reports that implicate this reaction as rate limiting in regard to CL generation (Eqns. 1–4) [11,12].

The use and the high sensitivity of the oxalate ester–hydrogen peroxide reaction for trace analysis is well documented [9–25]. However, complete ex-

0003-2670/89/$03.50

ploitation of the sensitivity limits of this system may not be realized until the solution reaction chemistry has been worked out. In this connection, and as a natural extension of earlier work on DNPO hydrolysis, this study was intended to examine the solution chemistry and kinetics of the pre-CL DNPO–H_2O_2 dark reaction [26].

EXPERIMENTAL

Materials

Bis(2,4-dinitrophenyl) oxalate (DNPO) was prepared as described by Rauhut et al. [1] or used as supplied (Sigma). 2,4-Dinitrophenol (DNP) (Aldrich) was separated from its water of hydration by dissolution in chloroform (Baker) and removal of the aqueous layer. The chloroform was evaporated and the DNP crystals were used as obtained. 9,10-Diphenylanthracene (DPA) (Aldrich), hydrogen peroxide (31.5%) (Fisher), acetonitrile (Baker, HPLC grade) and 2,4-dinitrophenyl acetate (DNPAc) (Kodak) were used as supplied. Distilled, deionized water was used when required.

Procedure

Reaction vessels were 10-ml glass-stoppered Erlenmeyer flasks. All glassware was washed with detergent, rinsed thoroughly with distilled water, rinsed with 50% nitric acid and again rinsed thoroughly with distilled water, followed by drying overnight in an oven. Stock solutions of hydrogen peroxide in acetonirile were prepared at 10-fold greater concentrations than used in any specific experimental reaction. Water was added, as necessary, to maintain a constant concentration (1.1 ± 0.1 M HaO).

DNPO was dissolved in acetonitrile at concentrations that were always 100 or more times lower than that of hydrogen peroxide or water. All reagent solutions were freshly prepared and allowed to reach reaction temperature (21.7°C unless indicated otherwise) in a constant-temperature water-bath (Forma Scientific 2095) prior to initiation of the reaction. A digital thermometer (Keithley 871) was used to monitor the water-bath temperature (± 0.2°C) throughout the experiments.

A reaction was started by gently adding one volume of the hydrogen peroxide–water stock solution to nine volumes of the DNPO solutions in the 10-ml flask. Complete mixing was ensured by mixing for 5 s in a vortex mixer. The reaction solution was transferred to a standard $1 \times 1 \times 4.5$ cm rectangular cell and placed in the spectrometer. All measurements were recorded beginning 1 min after the addition of the hydrogen peroxide solution to the DNPO solution. This procedure was used rather than mixing the two reactant solutions in the rectangular cell because of mixing problems associated with the latter method. Mixing the reactants in rigorously cleaned rectangular cells, regardless of the mixing method or carefulness of the mixing technique, resulted in unexplained

irreproducible data. However, when the same reactants were mixed in a 10-ml Erlenmeyer flask, under exactly the same conditions, reproducible data were obtained. In addition, mixing the two reactants by forcefully pipetting the hydrogen peroxide solution into the DNPO solution, by means of an adjustable volume pipetter (Gilson Pipetman), in either an Erlenmeyer flask or a rectangular cell, also resulted in irreproducible data. Other workers have reported the importance of the storage and mixing vessels for bis(2,4,6-trichlorophenyl) oxalate, hydrogen peroxide and a fluorophore [27]. All DNPO–H_2O_2 reactions were repeated in the presence of 1×10^{-5} M 9,10-diphenylanthracene (DPA) at 0.298 M hydrogen peroxide.

Absorbance measurements

A Varian 2200 spectrophotometer was used to measure the absorbances for DNPO and DNP, respectively, at 240 and 260 nm. Absorptivities of DNPO and DNP were measured daily and a calibration graph similar to that described previously was generated [26]. An appropriate dilution of the hydrogen peroxide stock solution was kept in the reference cell to negate the absorbance of hydrogen peroxide in the sample. DPA absorbance was accounted for in the same manner when necessary. At the sampling times of an experiment, 0.1 ml of the reaction mixture (or 0.2 ml for lower DNPO concentrations) was diluted to 2.0 ml in a quartz cuvette and the absorbance read. The calibration graph was used to develop a kinetic profile that was evaluated via procedures described extensively elsewhere [28].

Elemental analysis

Samples from two synthetic batches and one commercial lot of DNPO were analyzed by an independent laboratory (Atlantic Microlab, Norcross, GA) for carbon and hydrogen content (calculated, C 39.8, H 1.4; found, C 39.7, H 1.5%).

Melting point determination

A capillary melting-point apparatus (Arthur H. Thomas) was used to establish melting points for the DNPO samples described above (190–192, 185–190 and 185–188°C, respectively) and DNP (108–111°C). These values agree well with literature values [1,2] of 189–192 for DNPO and 112–114°C for DNP.

NMR analysis

A JEOL FX 270Q (270 MH_2) NMR spectrometer was used to obtain ^{13}C NMR spectra of DNPO and bis(2,4,6-trichlorophenyl) oxalate (TCPO). ^{13}C NMR spectral analysis of DNPO in either acetonitrile-d_3 or chloroform-*d* at room temperature was unsuccessful owing to the poor solubility of DNPO in these solvents. ^{13}C NMR spectra of TCPO in chloroform-*d* at 29, −9.6, −29.5 and −39.6°C were recorded.

RESULTS

Variation of DNPO concentration in excess hydrogen peroxide

The hydrogen peroxide concentration was 0.702 M with an initial DNPO concentration of 1.11×10^{-3} M. In order to determine the effect of the initial DNPO concentration, each experiment was repeated at two thirds of the initial DNPO concentration. The concentration- and time-normalized curves are superimposable [28] (Figs. 1 and 2). Plots of absorbance at 240 nm versus time showed only exponential decay and were not sigmoidal. The ratio of the absorbance at 240 nm to that at 260 nm decreased to a value equal to that of 2,4-dinitrophenol (DNP) over the time course of any single experiment.

Variation of excess hydrogen peroxide concentration

The experiment was repeated at hydrogen peroxide concentrations of 0.298, 0.224, 0.149, 0.112 and 0.0745 M with the water concentration adjusted to 1.1 M as in previous experiments. All semi-log arithmic plots revealed a biphasic loss of DNPO at each of the four temperatures examined. A typical example is shown in Fig. 3. The unweighted data were analyzed by the method of residuals to obtain rate constants for the fast and slow phases [29]. These data are given in Table 1. A plot of the observed rate constant versus hydrogen peroxide concentration was linear for each phase, indicating that both processes are first order with respect to hydrogen peroxide (Fig. 4). The lines converge and intersect the ordinate at a point corresponding to the rate constant for the hydrolysis reaction [26].

Addition of fluorophore (DPA)

No change in the kinetic profile was observed after the addition of DPA to the reaction mixture. The rate constants k_1 (0.192 min^{-1}) and k_2 (3.68×10^{-2}

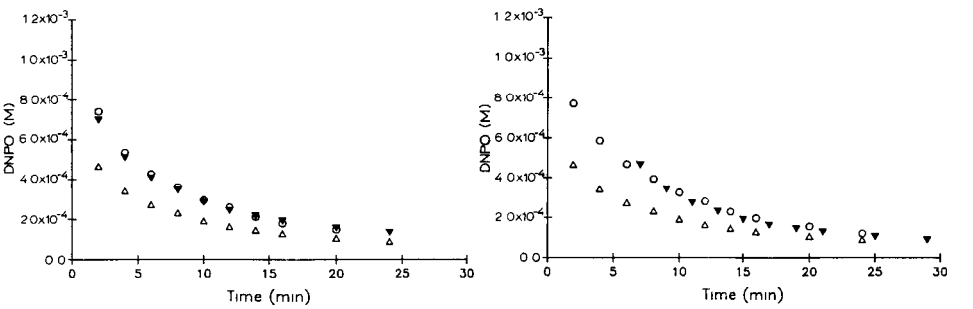

Fig. 1. DNPO concentration vs. time plot for (○) 1.11×10^{-3} M and (△) 0.74 M DNPO; (▼) = △ concentration multiplied by 3/2, to show superimposition.

Fig. 2. DNPO concentration vs. time plot. (○,△) as in Fig. 1; (▼) = △ shifted along the time axis.

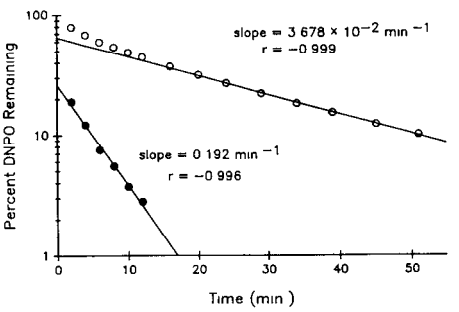

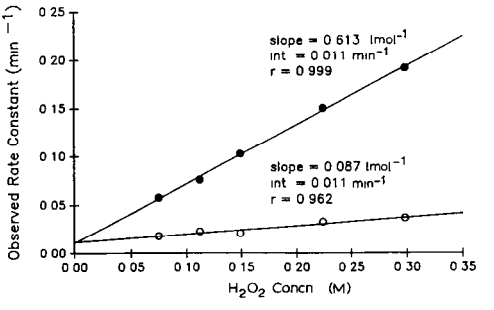

Fig. 3. Plot of biphasic degradation of DNPO (●) and residual points (○). DNPO=0.001 M; H_2O_2=0.298 M.

Fig. 4. Plot of observed rate constants of DNPO degradation for the fast and slow phases as a function of H_2O_2 concentration with a constant water concentration of 1.11 M. (●) k_1; (○) k_2.

TABLE 1

Rate constants at 21.7°C
(Rate constants ± 95% C.I. (in parentheses). n = number of points in terminal or residual regression line)

H_2O_2 (M)	k_2 (×100) (min^{-1})	r	n	k_1 (×100) (min^{-1})	r	n
0.298	3.68 (0.128)	−0.999	7	19.2 (2.32)	−0.996	6
0.224	3.28 (0.0436)	−0.999	7	15.0 (0.515)	−0.999	7
0.149	2.08 (0.0634)	−0.999	7	10.3 (1.19)	−0.995	7
0.112	2.29 (0.0755)	−0.999	8	7.59 (0.533)	−0.999	6
0.0745	1.81 (0.0401)	−0.999	6	5.77 (0.420)	−0.999	5

min^{-1}) lie within a 95% confidence interval of those determined without DPA present. The CL reaction was also monitored under the same conditions and showed a first-order decay with k_{obs} = 33.6 min^{-1}.

Effect of temperature

The experiment with 0.224 M hydrogen peroxide was also done at 11.9, 31.6 and 41.5°C. The results (Table 2), when fitted to the Arrhenius equation, gave activation energies of 27.1 and 21.7 kJ mol^{-1} for the fast and slow phases, respectively.

^{13}C NMR studies

The ^{13}C NMR spectra recorded for TCPO in chloroform-*d* showed no temperature dependence. All peaks present at room temperature (23°C) remained

TABLE 2

Rate constants in 0.224 M hydrogen peroxide
(Rate constants ± 95% C.I. (in parentheses). n = number of points in terminal or residual regression line)

Temperature (°C)	k_1 (×100) (min^{-1})	r	n	k_1 (×100) (min^{-1})	r	n
11.9	2.54 (0.125)	−0.999	6	9.41 (0.502)	−0.999	6
31.6	4.40 (0.0632)	−0.999	9	20.8 (0.793)	−0.999	6
41.5	6.01 (0.174)	−0.999	7	27.8 (1.86)	−0.999	5

unchanged at −9.6, −29.5 and −39.6°C. Particular attention was given to the carbonyl peak at 152.07 ppm. However, no splitting of the peak into two compounds was observed.

DISCUSSION

Variation of DNPO in excess hydrogen peroxide

The DNPO–H_2O_2 reaction follows first-order kinetics since the concentration-normalized concentration versus time plots were superimposable (Fig. 1). The results indicate the presence of only first- or pseudo-first-order reactions regardless of the complexity of the reaction [28]. The time-normalized concentration versus time plots were also superimposable, showing that no intermediate(s) or product(s) affect(s) the reaction rate during the time course of the experiments [28] (Fig. 2).

Variation of excess hydrogen peroxide concentration

Semi-logarithmic plots of DNPO concentration versus time were biphasic at each of the six hydrogen peroxide concentrations and four temperatures examined (Fig. 3). This result is not expected for a simple first-order reaction and shows that the reaction is more complex than the data in Figs. 1 and 2 reveal.

In the following discussion three possible reasons for the biphasic plots in Fig. 3 are examined: the experimental method does not distinguish between DNPO isomers; intermediates may be confounding the experimental results; hydrolysis is competing with the hydrogen peroxide reaction, but at a slower rate.

In the first instance, the experimental method may not distinguish between DNPO isomers that exist in equilibrium ($DNPO = DNPO_1 + DNPO_2$), where both $DNPO_1$ and $DNPO_2$ degrade to produce the primary reaction product DNP, each at a different rate ($k_1 > k_2$). Under these conditions the reaction

scheme would consist of two parallel first-order reactions with a common product, and with the reactants in equilibrium (Eqn. 5).

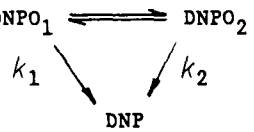

(5)

For this process, the rate equation cannot be condensed, and an exponential term for each isomer would appear in the integrated equation:

$$[\mathrm{DNPO}] = [\mathrm{DNPO_1}]\exp(-k_1 t) + [\mathrm{DNPO_2}]\exp(-k_2 t)$$

Biphasic semilogarithmic plots have been reported for the hydrolysis of some tertiary alkyl chlorides [30,31]. This result was attributed to stereoisomers that were hydrolyzed at different rates. The initial linear and terminal portions of these plots were analyzed by the method of residuals and simple extrapolation, in order to obtain rate constants for the fast and slow reactions, respectively. In this work the same procedure as shown in Fig. 3 and Table 1 was used (k_1 and k_2 are the rate constants for the fast and slow phase, respectively). In addition to the above studies, conformational and rotational isomers are also known to undergo reactions at different rates [32–37]. For oxalate esters, even those as conformationally bulky as DNPO, conformational or rotational isomers are likely owing to reports that bis(diethyl) oxalate exists either as a mixture of non-planar [38] or planar [39–41] *cis* and *trans* isomers.

Preliminary results of a conformational analysis of DNPO using the TRIPOS molecular mechanics force-field computer program indicate the existence of two distinct populations of conformers corresponding to the *cis* and *trans* isomers [42]. The calculations indicate that the *trans* state is not only more stable but also is more highly populated than the *cis* state. If the calculations are correct, then the terminal slow phase of the curve in Fig. 3 describes *trans*-isomer degradation and the initial phase *cis*-isomer degradation. This agrees with the experimental data since extrapolation of the terminal and residual lines in Fig. 3 to the ordinate gives a population ratio of ca. 7:3 in favor of the *trans* isomer. The calculations also indicate a rotational barrier between the two isomers of about 10–12 kJ mol^{-1}. This value compares favorably with the value of 11.7 kJ mol^{-1} for the *cis–trans* isomerization of oxalyl chloride [43,44]. Further studies utilizing an ab initio quantum mechanical program are currently in progress.

^{13}C NMR spectral studies using TCPO indicate that it and perhaps other oxalate esters such as DNPO exist as a mixture of non-planar *cis* and *trans* isomers as reported for bis(diethyl) oxalate [38]. Depending on the degree of non-planarity, each of the two isomers may be in a staggered conformation such that the carbonyl functional groups are spectroscopically indistinguishable. This would explain why the ^{13}C NMR carbonyl peak at 152 ppm is not

split. Molecular models substantiate this possibility, but more rigorous molecular modeling computations must be completed in order to validate it.

A second possible reason for the biphasic plots in Fig. 3 is that a DNPO- or DNP-like intermediate is confounding the experimental results. Some possible intermediate structures (IM) are shown in Fig. 5 [6,12]. As in earlier work, DNPAc was used as a model compound for DNPO-like intermediates (structure 1, Fig. 5) [26]. Its UV absorption spectrum is identical with that of DNPO (structure 2, Fig. 5) except that its absorptivity is half that of DNPO. In this connection, structure 3 would be expected to have an absorption spectrum and absorptivity almost identical with those of DNPAc, by analogy with the phenylacetic acid and phenylchloroacetic acid esters, which have virtually identical absorption spectra and absorptivities [45]. Then structure 4 would appear spectroscopically as a composite of DNPAc and DNP. Both structures 5 and 6 would have spectra like that of DNP, but structure 5 would have twice the absorbance of structure 6.

Using this model, two first-order series reaction schemes, each containing two steps can be used to generally describe the reaction:

$$\text{DNPO} \xrightarrow{k_1} \text{IM} + \text{DNP} \qquad (6)$$

$$\text{IM} \xrightarrow{k_2} \text{DNP} + \text{products}$$

$$\text{DNPO} \xrightarrow{k_1'} \text{IM}' + 2\text{DNP} \qquad (7)$$

$$\text{IM}' \xrightarrow{k_2'} \text{products}$$

In Eqn. 6, if structure 3 (Fig. 5) is the IM, then the scheme is as written. If structure 4 is the IM, DNP is not an actual product but remains attached to the skeletal remains of DNPO. The spectrum obtained would be the same in each instance. In Eqn. 7, if 2DNP were produced then the IM′ must be

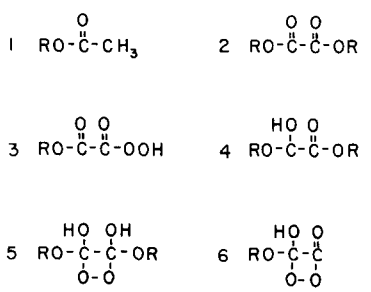

Fig. 5. (1) DNPAc; (2) DNPO; (3) and (4) possible DNPO-like intermediates; (5) and (6) possible DNP-like intermediates; R is 2,4-dinitrophenol.

dioxetanedione (C_2O_4). If structure 5 is the IM′, then no DNP would be produced in this first step and

$$\begin{aligned} &\text{DNPO} \longrightarrow \text{IM}' \\ &\text{IM}' \longrightarrow 2\text{DNP} + \text{products} \end{aligned} \tag{8}$$

If structure 6 is the IM′, then 1DNP would be produced in the first step and

$$\begin{aligned} &\text{DNPO} \longrightarrow \text{IM}' + \text{DNP} \\ &\text{IM}' \longrightarrow \text{DNP} + \text{products} \end{aligned} \tag{9}$$

The spectrum obtained would be the same in all three instances.

In Eqn. 6, if $k_1 \geqslant k_2$ and IM is a DNPO-like intermediate (structures 3 and 4, Fig. 5), then appreciable amounts of IM would be produced. This reaction scheme can be computer simulated using absorptivities for DNPO and DNP and the value for DNPAc for IM to construct simulated calibration graphs of A_{240}/A_{260} (A = absorbance) (λ_{max} for DNPO and DNP, respectively) vs. DNPO concentration. The comparative concentrations of DNPO, IM and DNP during the course of a reaction, real or simulated, depend on the ratio $k_1 : k_2$. The ratios chosen were 1:1, 1:2, 1:3, ..., 1:10, 1:20, 1:30, ..., 1:100, 1:200, 1:300, ..., 1:1000 and the inverse. Using these values, 73 simulated calibration graphs of A_{240}/A_{260} vs. DNPO concentration were constructed. Simulated values for DNPO concentration were obtained from these graphs by using experimental absorbance measurements. These were used to construct log (DNPO concentration) vs. time plots (time values corresponded to experimental absorbance values). Evaluation of the latter for both linearity and zero-time intercepts did not yield statistically valid results. Therefore, a series reaction with DNPO-like intermediates was ruled out as an explanation for the biphasic plots in Fig. 3.

For the case in Eqn. 6 where $k_1 \geqslant k_2$ and IM is a DNP-like intermediate (structures 5 and 6, Fig. 5) no matter what values were assigned to k_1 and k_2 the experimental data would give linear log (DNPO concentration) vs. time plots with an intercept on the ordinate corresponding to the initial DNPO concentration. This was not observed, as seen in Fig. 3.

The computer simulation studies strongly indicate that the DNPO–H_2O_2 reaction does not proceed by a first-order series reaction. In addition, it does not produce either DNPO- or DNP-like aryl intermediates. The latter point agrees with a statement by Mohan [46] that the key intermediate in the oxalate ester CL reaction does not have the aryl group attached. Further substantiation of the lack of aryl intermediates is given by the result that plots of DNPO absorbance maxima vs. time demonstrate only an exponential decline. This means that an absorbing intermediate cannot be present in this wavelength region because it would cause these plots to be sigmoidal [28]. It should be noted that the most often proposed key cyclic intermediate, dioxetanedione

(C_2O_4), has not yet been isolated. Its existence is indirectly supported by the result that no absorbing aryl intermediate could be detected in the UV region examined. Equation 7 describes this possibility where IM′ is a non-absorbing intermediate.

A third possibility for the biphasic plots in Fig. 3 is that the slow or terminal phase is due to the hydrolysis reaction. Since water is present in the reaction, the hydrolysis rate constant is a component of the observed rate constant ($k_{obs.} = k_{H_2O} + k_{H_2O_2}$). If the slow phase was due to the hydrolysis reaction, the slope of the $k_{obs.}$ vs. hydrogen peroxide concentration plot (Fig. 4) for the slow phase should be zero, since the water concentration was held constant at 1.1 M. A *t*-test for this slope resulted in $k_2 > 0$ at $\alpha = 0.05$. In addition, when each line in Fig. 4 was extrapolated to the ordinate, they both intersected at the same point, which corresponds to the rate constant for the hydrolysis reaction [26]. Further, it would be difficult to support the notion that only hydrolysis was responsible for the slow phase because hydrogen peroxide is still present in great excess at the later experimental time points. For these reasons, the possibility that the terminal phase was due to hydrolysis was ruled out.

The data in Table 1 and Fig. 4 show that the pre-CL reaction, like the CL reaction, is dependent on hydrogen peroxide concentration [11,23]. However, the initial fast reaction is more susceptible to changes in hydrogen peroxide concentration than is the terminal reaction. In the former, an increase in hydrogen peroxide concentration causes a 3.3-fold increase in k_1 as opposed to a 2-fold increase in k_2 (Table 1). The dissimilarity in reactivity may not only indicate the presence of conformationally different DNPO isomers, but also refutes the idea that hydrolysis is responsible for the slower terminal phase (Fig. 3).

The possibility that DNPO may exist in two conformations could cause the results of Alvarez et al. [6] to be interpreted differently. Their CL system consisting of hydrogen peroxide, bis(2,4,6-trichlorophenyl) oxalate (TCPO) and triethylamine (TEA), could be adjusted to show two distinct pulses of chemiluminescent intensity by varying the catalyst concentration (TEA). Using a series reaction model they proposed a scheme that included, as necessary, the production of a non-CL intermediate, Z, from a CL-yielding intermediate, X. Z is subsequently converted to a CL-yielding intermediate, Y (X...Z...Y). Biphasic decay of the oxalate (assuming like behavior of DNPO and TCPO) could also be responsible for these pulses, one pulse from the energy transfer intermediate derived from each conformer. Z would not be required to be converted from X, but would simply be starting material (i.e., one of the oxalate conformers).

Addition of fluorophore

There are conflicting literature reports concerning the effect of fluorophore addition to an ongoing oxalate ester–hydrogen peroxide reaction. One study

[1] reports that the addition of the fluorophore DPA catalyzes the decomposition of the reactive intermediate created during the reaction. Another [8] reports that these results cannot be duplicated under the same experimental conditions. The results of this work show that DPA does not catalyze or otherwise affect the pre-CL DNPO–H_2O_2 reaction. This indicates that if DPA or other similar fluorophores do affect the reaction rate, it must occur later in the reaction scheme than the initial pre-CL DNPO–H_2O_2 reaction. The obvious conclusion is that DPA interacts only with the reactive intermediate. In addition, the result that CL decay from the DNPO–H_2O_2–DPA reaction (Eqn. 4) has a rate constant ($k_{obs.} = 33.6\ min^{-1}$) that is 175-fold greater than that for the fastest DNPO–H_2O_2 reaction reported in Table 1 ($0.192\ min^{-1}$, under the same experimental conditions) indicates that the pre-CL reaction (Eqn. 1) is also the rate-limiting step in the proposed reaction scheme (Eqns. 1–4). This is in agreement with two other studies [11,12] that reported the same conclusion obtained by different methods and with different oxalate esters.

Effect of temperature

The DNPO–H_2O_2 reaction demonstrates a relatively small temperature effect, approximately a 2.5-fold increase for a 30°C rise in temperature. This result and the low activation energies are typical of reactions that go to completion in a period from minutes to hours at room temperature [28]. The energies of activation reported for the reaction (27.1 and 21.7 kJ mol^{-1}) are almost identical with that for DNPO hydrolysis (24.5 kJ mol^{-1}). However, a meaningful direct comparison is impossible since the two reaction systems are not identical.

The authors thank Dr. E.W. Taylor for the molecular mechanics force field analysis.

REFERENCES

1 M.M. Rauhut, L.J. Bollyky, B.G. Roberts, M. Loy, R.H. Whitman, A.V. Iannotta, A.M. Semsel and R.A. Clarke, J. Am. Chem. Soc., 89 (1967) 6515.
2 F. McCapra, Prog. Org. Chem., 8 (1973) 231.
3 K.-D. Gunderman and F. McCapra, Chemiluminescence in Organic Chemistry, Springer, Berlin, Heidelberg, 1987, Chap. VI.
4 M.M. Rauhut, B.G. Roberts, D.R. Maulding, W. Bergmark and R. Coleman, J. Org. Chem., 40 (1975) 330.
5 C.D. Dowd and D.B. Paul, Aust. J. Chem., 37 (1984) 73.
6 F.J. Alvarez, N.J. Parekh, B. Matuszewski, R.S. Givens, R. Higuchi and R.L. Schowen, J. Am. Chem. Soc., 108 (1986) 6435.
7 M.M. Rauhut, Acc. Chem. Res., 2 (1969) 80.
8 E.H. White, P.D. Wildes, J. Wiecko, H. Doshan and C.C. Wei, J. Am. Chem. Soc., 95 (1973) 7050.

9 K. Honda, J. Sekino and K. Imai, Anal. Chem., 55 (1983) 940.
10 S. Kobayashi and K. Imai, Anal. Chem., 52 (1980) 424.
11 G. Orosz, Tetrahedron, 45 (1989) 3493.
12 C.L.R. Catherall, T.F. Palmer and R.B. Cundall, J. Chem. Soc., Faraday Trans. 2, 80 (1984) 823, 837.
13 R. Weinberger, C.A. Mannan, M. Cerchio and M.L. Grayeski, J. Chromatogr., 288 (1984) 445.
14 G.J. De Jong, N. Lammers, F.J. Spruit, M. Frei and U.A.Th. Brinkman, J. Chromatogr., 353 (1986) 249.
15 M.L. Grayeski and A.J. Weber, Anal. Lett., 17(A13) (1984) 1539.
16 K.W. Sigvardson and J.W. Birks, Anal. Chem., 5 (1983) 432.
17 N. Hanaoko, R.S. Givens, R.L. Schowen and T. Kuwang, Anal. Chem., 60 (1988) 2193
18 G. Mellbin, J. Liq. Chromatogr., 6 (1983) 1603.
19 K. Honda, K. Miyaguchi and K. Imai, Anal. Chim. Acta, 177 (1985) 103.
20 G.J. De Jong, N. Lammers, F.J. Spruit, U.A.Th. Brinkman and R.W. Frei, Chromatographia, 18 (1984) 3, 129.
21 J.L. Mullin and M.L. Grayeski, Anal. Chem., 56 (1984) 1046.
22 A.J. Weber and M.L. Grayeski, Anal. Chem., 136 (1984) 277.
23 M.L. Grayeski and W.R. Seitz, Anal. Biochem., 136 (1984) 277.
24 M.S. Abdel-Latif and G.G. Guilbault, Anal. Chem., 60 (1988) 2671.
25 A.C. Capomacchia, R.N. Jennings, S.M. Hemingway, P. D'Souza, W. Prapaitrakul and A. Gingle, Anal. Chim. Acta, 196 (1987) 305.
26 R.N. Jennings and A.C. Capomacchia, Anal. Chim. Acta, 205 (1988) 207.
27 N. Hanaoko, Anal. Chem., 61 (1989) 1298.
28 R. Schmid and V.N. Sapunov, Non-Formal Kinetics, Verlag Chemie, Deerfield Beach, FL, 1982.
29 M. Gibaldi and D. Perrier, Pharmacokinetics, Dekker, New York, 1982, p. 433.
30 H.C. Brown and R.S. Fletcher, J. Am. Chem. Soc., 71 (1949) 1845.
31 H.C. Brown and R.S. Fletcher, J. Am. Chem. Soc., 73 (1951) 1317.
32 R.T. Morrison and R.N. Boyd, Organic Chemistry, 3rd edn., Allyn and Bacon, Boston, 1973.
33 E.L. Eliel, Experientia, 9 (1953) 91.
34 S. Winstein and N.J. Holness, J. Am. Chem. Soc., 77 (1955) 5562.
35 M. Nakamura, N. Nakamura and M. Oki, Bull. Chem. Soc. Jpn., 50 (1977) 1097
36 M. Oki and R. Saito, Chem. Lett., (1981) 649.
37 R. Saito and M. Oki, Bull. Chem. Soc. Jpn., 55 (1982) 3267.
38 M.J. Aroney, D. Izsak and R.J.W. LeFevre, J. Chem. Soc., (1962) 3997.
39 S.-I. Mizushima, Internal Rotation and Molecular Configuration, Academic, New York, 1954, p. 75.
40 J. Miyazawa and J. Kurantani, J. Chem. Soc. Jpn., 72 (1951) 804.
41 J. Miyazawa, J. Chem. Soc. Jpn., 75 (1954) 540.
42 Sybyl, Molecular Modeling Software, Version 5.1, Tripos Association, St. Louis, MO, 1988.
43 B.D. Saksena and R.E. Kagarise, J. Chem. Phys., 19 (1951) 987.
44 R.E. Kagarise, J. Chem. Phys., 19 (1953) 1615.
45 Sadtler Standard Reference Spectra, Ultraviolet Collection, Sadtler Research Laboratories, Richmond, CA, 1980.
46 A.G. Mohan, Chemalog Hi-Lites, 9 (1985) 9.